IEEE Access
Multidisciplinary | Rapid Review | Open Access Journal

Received April 3, 2022, accepted April 25, 2022, date of publication April 28, 2022, date of current version May 5, 2022.

Digital Object Identifier 10.1109/ACCESS.2022.3171050

Coherent Optical OFDM With Index Modulation for Long-Haul Transmission in Optical Communication Systems

AHMET GÜNER
Department of Electrical and Electronics Engineering, Bingöl University, 12000 Bingöl, Turkey
e-mail: aguner@bingol.edu.tr

ABSTRACT In this paper, it is proposed to enhance coherent optical orthogonal frequency-division multiplexing (OFDM) system by using index modulation in terms of bit error rate (BER) and spectral efficiency for different levels of the fiber nonlinearity. In the coherent optical OFDM with index modulation system (CO-OFDM-IM), the information is conveyed not only through activated subcarriers but also by indices of the active subcarrier that are dynamically updated at the transmitted symbol rates. Unlike the conventional coherent optical OFDM (CO-OFDM) system, adjusting the number of the active subcarriers in the CO-OFDM-IM system provides improved BER performance and reduction the signal peak-to-average-ratios, when the fiber nonlinearity becomes significant. The simulation results illustrate that the proposed CO-OFDM-IM system has better BER performance when the proposed CO-OFDM-IM system and the CO-OFDM system have similar spectral efficiency. Also, the CO-OFDM-IM system can provide better spectral efficiency than the CO-OFDM system at the low-to-medium order modulation such as BPSK, QPSK, and 16QAM.

INDEX TERMS Coherent optical communications, OFDM, OFDM with index modulation, spectral efficiency.

I. INTRODUCTION

Optical communication is a promising complementary technique to radio-frequency (RF) communication for long-haul transmission such as radio-over-fiber (RoF). RoF technology has been considered as an enabling solution for the future broadband wireless access networks, due to its attractive features such as high bandwidth, extended coverage, and simplified base station [1]. Also, with the expansion of the 5G network construction scale and the innovative development of the industrial internet, the construction of the optical network is marching towards higher speed, large capacities, and long distances [2]. Nowadays, the coherent optical communication system plays an important role in the communication field as well as improves spectral efficiency and capacity [3]. For example, the ease of optical channel effects compensation together with high spectral efficiency are the major advantages of coherent optical orthogonal frequency-division multiplexing (CO-OFDM). Therefore CO-OFDM systems are proposed for long-haul transmission [4].

The associate editor coordinating the review of this manuscript and approving it for publication was Tianhua Xu.

In 5G and beyond, especially 6G, it has been investigated about what are the best suitable waveforms. Various modulation techniques, such as the filter bank based multicarrier (FBMC) [5], windowed-OFDM (W-OFDM) [6], filtered-OFDM (F-OFDM) [7] and generalized frequency division multiplexing (GFDM) [8], have been proposed for both the obtaining of high spectral efficiency and the using of them in low power applications. Among possible candidates, orthogonal frequency-division multiplexing (OFDM) is already used in most modern communication systems, including 4G, 5G, and Wi-Fi. The main benefits of OFDM are a very efficient hardware implementation and single-tap equalization at the receiver. Also, OFDM has been widely used in both wireless and optical communication systems.

Index modulation (IM) is a technique inspired by the idea of a spatial modulation scheme that is capable of achieving high spectral efficiency by way of allowing transmitting additional bits compared with the conventional modulation techniques [9]. The IM has been intensively investigated in different communication systems such as multi-carrier systems [9], MIMO systems [10], molecular

communication [11], millimeter-wave transmission [12], visible light communication, [13]–[15] and polar codes [16].

In 2013, Başar *et al.* proposed firstly OFDM with index modulation (OFDM-IM) scheme [9]. OFDM-IM both provides innovative ways [8], [17]–[22] to convey information compared to conventional OFDM and offers advantages in terms of spectral and energy efficiency [23]. In OFDM-IM, the information is conveyed not only by the active subcarriers, which are activated to carry constellation symbols but also by the indices of the active subcarriers, which are used for the transmission of the additional binary information. So OFDM-IM offers a trade-off between spectral efficiency and system performance by the adjustment of the number of active subcarriers [9].

Higher launch power levels are desirable to extend the reach of transmission in long-haul links. However, in long-haul CO-OFDM, significant distortions are due to the fiber nonlinearity. Higher input power levels result in performance degradation due to the effect of the fiber nonlinearity [24]. To improve spectral efficiency and use the advantages of OFDM-IM compared to OFDM, OFDM-IM can be employed in coherent optical communication systems.

The effect of fiber nonlinearity causes nonlinear interference between subcarriers caused by adjacent subcarriers in OFDM. Therefore, in this paper, it is aimed to reduce the number of active subcarriers at the same spectral efficiency in order to mitigate the fiber nonlinearity effect. While index modulation provides the possibility to transmit additional information bits using subcarrier indices in OFDM, some subcarriers become inactive. So, index modulation is proposed to reduce the number of nonlinear interfering subcarriers by using inactive subcarriers and to enhance BER performance at the same spectral efficiency for coherent optical OFDM systems.

Simulation results demonstrate that the proposed coherent optical OFDM-IM can improve the spectral efficiency, and the BER performance can be enhanced at the same spectral efficiency in comparison with conventional coherent optical OFDM when the fiber nonlinearity is considered.

II. COHERENT OPTICAL OFDM WITH INDEX MODULATION SYSTEM

A. TRANSMITTER

The block diagram of the proposed coherent optical OFDM with index modulation (CO-OFDM-IM) system is depicted in Fig. 1. For the transmission of each OFDM symbol, a variable number of the information bits enter the transmitter of the CO-OFDM-IM system. These bits are firstly split into OFDM subblocks. G is the total number of the OFDM subblocks. Each OFDM subblock contains subcarriers of length $n = N_{FFT}/G$, where N_{FFT} is the size of the fast Fourier transform (FFT). $p = p_1 + p_2$ bits is mapped to an OFDM subblock of length n. The mapping operation is not only performed by means of the modulated symbols, but also by the indices of the subcarriers. The indices of k active subcarriers are determined by a selection procedure based on the first p_1 bits of the incoming p-bit sequence for transmitting additional information bits. The number of additional information bits can be given by

$$p_1 = \left\lfloor \log_2(C(n,k)) \right\rfloor \tag{1}$$

where $\lfloor . \rfloor$ is the floor operation and $C(\cdot)$ is the combinatorial operation.

For each g^{th} OFDM subblock ($g = 1, 2, \ldots, G$), p_2 bits of the incoming p-bit sequence are mapped onto the M-ary signal constellation, where M is the constellation size, in order to determine the data symbols that are transmitted over the k active subcarriers. The number of the remaining p_2 bits can be given by

$$p_2 = k\left(\log_2(M)\right) \tag{2}$$

p_1 bits are sent to an index selector to generate indices which indicate to k active subcarriers. The index selection is implemented by using combinatorial method. The combinational number system of degree k provides a one-to-one mapping relationship with the set of k active subcarrier indices [9]. For any n and k values, the natural number $Z \in [0, C(n,k) + 1]$ can be presented by a unique descending sequence $J = \{j_k, \ldots, j_1\}$, which takes elements from the set according to the following equation:

$$Z = C(j_k, k) + \cdots + C(j_2, 2) + C(j_1, 1) \tag{3}$$

where $j_k > \cdots > j_1 \geq 0$ and $j_k, \ldots, j_1 \in \{0, \ldots, n-1\}$ [9]. The obtained J indices sequence from input p_1 additional information bits can be explained by Algorithm 1 [25].

Algorithm 1 Obtain J Indices Sequence From Input p_1 Bits

1: **Input**: The binary sequence of p_1 bits, the number of subcarriers n, the number of active subcarriers k
2: **Initialization**: Convert p_1 bits into a decimal number Z, $jj \leftarrow n$
3: **for** $i = k : -1 : 1$ **do**
4: **repeat**
5: $jj \leftarrow jj - 1$
6: ComCoef $\leftarrow$ C(jj, i)
7: **until** ComCoef $\leq$ Z
8: $j_i \leftarrow jj$
9: Z $\leftarrow$ Z$-$ ComCoef
10: **end for**
11: **return** array j_i

To make easy understanding, as an example of how active or inactive subcarriers are determined, for $n = 4$ and $k = 2$, the number of p_1 additional information bits is calculated using (1) that $p_1 = \left\lfloor \log_2(C(4,2)) \right\rfloor = 2$. The p_1 bits are first converted to a decimal number Z. Then the combinational number system provides a one-to-one mapping between natural number Z and k-combinations (see Algorithm 1 to find the k-combination for a given number Z).

After J indices sequence is obtained from input p_1 additional information bits, the symbol in the inactive subcarriers is setted to zero. In Table 1, it is shown the subblocks obtained for different p_1 additional information bits. s_a and s_b are transmitted constellation symbols on active subcarriers.

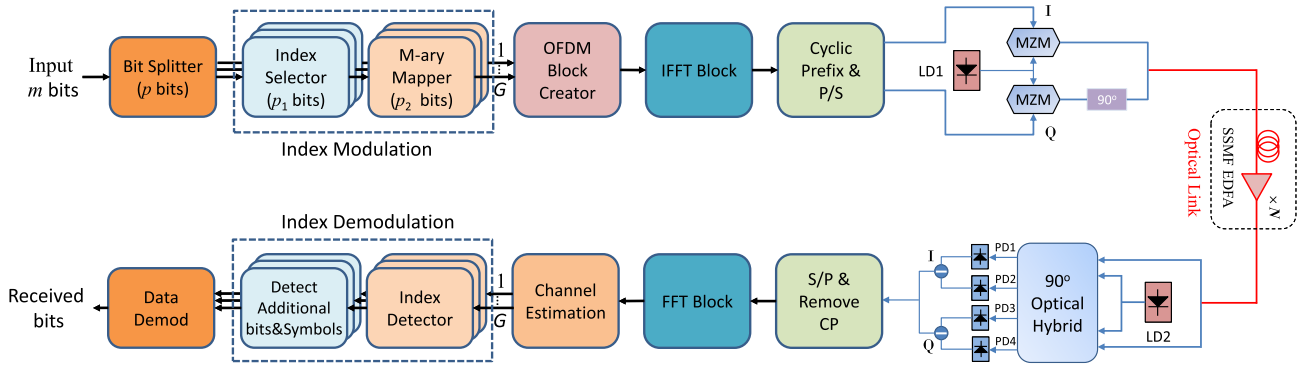

FIGURE 1. The block diagram of the proposed coherent optical OFDM-IM system.

TABLE 1. The mapping relationship between p_1 bit sequences and J active subcarrier indices for $n = 4, k = 2$ and $p_1 = 2$.

p_1 bits	Decimal number	k-combination	J indices sequence	Subblocks
[0 0]	0	$C(1,2)+C(0,1)$	[1,0]	$[s_a\ s_b\ 0\ 0]$
[0 1]	1	$C(2,2)+C(0,1)$	[2,0]	$[s_a\ 0\ s_b\ 0]$
[1 0]	2	$C(2,2)+C(1,1)$	[2,1]	$[0\ s_a\ s_b\ 0]$
[1 1]	3	$C(3,2)+C(0,1)$	[3,0]	$[s_a\ 0\ 0\ s_b]$

The g^{th} OFDM subblock can be represented as

$$\{X_g\}_{i=1,\ldots,n} = \begin{cases} s_g(i), & i \in J_g \\ 0, & \text{otherwise} \end{cases} \tag{4}$$

where $s_g(i)$ are independently obtained from a M-ary signal constellation. After concatenating X_g, the equivalent time-domain signal can be calculated by using the inverse Fourier transform as follows

$$v(t) = \frac{1}{\sqrt{T}} \sum_{g=1}^{G} \sum_{i=1}^{n} X_g(i) e^{j2\pi f_{g,i} t}, \quad 0 \le t \le T \tag{5}$$

where $f_{g,i}$ is the i^{th} subcarrier frequency in the g^{th} OFDM subblock and T is the time duration of a OFDM-IM symbol. Then parallel to serial conversion and Cyclic prefix (CP) insertion are followed.

The electrical signal obtained after the inverse conversion process is converted into a transmitted optical signal with two optical IQ modulators (Mach-Zehnder Modulator - MZM) [26].

B. OPTICAL CHANNEL

The optical channel includes many Standart Single Mode Fiber (SSMF) lengths. For SSMF, within each span, the nonlinear Schrodinger equation (NLSE) models loss, chromatic dispersion (CD), and nonlinear effects as

$$\frac{\partial E(z,t)}{\partial z} = (D+N)E(z,t) \tag{6}$$

where E is the complex light envelope of the received signal after a fiber distance of z km. D is the linear part for linear effects (CD and attenuation) and N is the nonlinear part, which is given by:

$$D = -\frac{j}{2}\beta_2 \frac{\partial^2}{\partial t^2} - \frac{\alpha}{2} \tag{7}$$

$$N = j\gamma |E(z,t)|^2 \tag{8}$$

$$\gamma = \frac{2\pi n_2}{\lambda_c A_{eff}} \tag{9}$$

where α is the attenuation factor, β_2 is the group velocity dispersion parameter, γ is the nonlinearity coefficient, n_2 is the nonlinear-index coefficient, λ_c is the center wavelength and A_{eff} is the effective core area [27]. At the end of each span, the optical signal is amplified to compensate for fiber losses by an EDFA.

C. RECEIVER

At the receiver, the received optical signal after transmission through the optical channel is converted to an electrical signal by a local oscillator laser (LO) by passing through a 90° optical hybrid. The optical signal interferes with the local oscillator laser, which usually has the same frequency as the transmitter laser in the 90° optical hybrid. In order to detect both real and imaginary parts, the input signal is mixed with the real part of the local oscillator laser in one branch and the imaginary part in the other branch through the 90° phase shift between the signal and the local oscillator laser.

At the CO-OFDM-IM receiver after removing CP and implementing the FFT operation, it is followed by a channel estimation operation. To be able to equalize the received signal in the frequency domain, it is important to estimate the channel frequency response. $\hat{X}_g(i)$ is the received vector for the g^{th} OFDM subblock after FFT operation, which is given by

$$\hat{X}_g(i) = H_g(i)X_g(i) + W_g(i), \quad i = 1, \ldots, n \tag{10}$$

where $H_g(i)$ and $W_g(i)$ denote respectively the channel frequency response and the zero-mean complex additive white Gaussian noise (AWGN) with variance N_0 on the i^{th} subcarrier of the g^{th} OFDM subblock. PN sequence block, which is suitable for the fiber optical channel with slow variation,

is used for the channel estimation, which is given by

$$\hat{H}_g(i) = \frac{\hat{X}_g^{PN}(i)}{X_g^{PN}(i)}, \quad i = 1, \ldots, n \tag{11}$$

where $\hat{X}_g^{PN}(i)$ and $X_g^{PN}(i)$ are the PN sequence signal on the i^{th} subcarrier of the g^{th} OFDM subblock at the receiver and the transmitter respectively.

It needs to detect both the indices of active subcarriers and the corresponding additional information bits. The index detector is used to detect indices of active subcarriers from each OFDM subblock. The maximum likelihood (ML) detector of the CO-OFDM-IM system searches all combinations of subcarrier indices and the constellation points in order to a joint decision on the indices of active subcarriers and the transmitted symbols for each OFDM subblock.

The searching space of the ML detection per bit is given by the order of $O\left(C(n,k) + M^k\right)$. Since the complexity increases exponentially with increasing k values, the optimal ML detector has high complexity. To achieve near optimal performance, the low-complex posteriori probability detection (PPD) method have been proposed [8].

The PPD detector of CO-OFDM-IM gives the logarithm of the ratio of a posteriori probabilities of frequency domain signals by considering the case that the values are either non-zero or zero [9]. For the g^{th} OFDM subblock, the PPD detector provide the probability of the active status of the corresponding index i with $i = 1, 2, \ldots, n$ given by;

$$\lambda_g(i) = \ln \frac{\sum_{m=1}^{M} P\left(X_g(i) = Q_m \mid \hat{X}_g(i)\right)}{P\left(X_g(i) = 0 \mid \hat{X}_g(i)\right)} \tag{12}$$

where Q_j is the element of a M-ary signal constellation. The larger the value of $\lambda_g(i)$, the higher the probability that the corresponding i is an active subcarrier. Using Bayes formula, (12) can be expressed as

$$\lambda_g(i) = \ln(k) - \ln(n-k) + \frac{\left|\hat{X}_g(i)\right|^2}{\sigma_k^2} + \ln\left(\sum_{m=1}^{M} \exp\left(-\frac{1}{\sigma_k^2}\left|\hat{X}_g(i) - H_g(i)Q_m\right|^2\right)\right) \tag{13}$$

After obtaining all a posteriori probabilities based on (13), for each OFDM subblock, the receiver decides on k active indices $(\hat{J})$ having maximum posteriori probabilities. After determining the k active indices, the additional information bits and the data symbols can be easily decided.

It takes the active indices sequences from the index detector and performs a summation of the k-combination coefficients (Algorithm 2) for each OFDM subblock. After calculating decimal number $\hat{Z}$, the additional information bits can be decided with a decimal-to-binary converter. Transmitted symbols at sets of M-ary signal constellation (Q) on k active subcarriers are estimated as

$$\hat{P}_g(i)\Big|_{i=1}^{k} = \arg\min_{Q_m \in Q} \left|\hat{X}_g(i) - \hat{H}_g(i)Q_m\right|^2 \tag{14}$$

Algorithm 2 Obtain Decimal Number $\hat{Z}$ From the Indices Sequence $\hat{J}$

1: **Input**: The indices sequence $\hat{J} = \left\{\hat{j}_k, \ldots, \hat{j}_1\right\}$,
the number of subcarriers n, the number of active subcarriers k
2: $\hat{Z} \leftarrow 0$
3: **for** $i = 1 : k$ **do**
4: ComCoef $\leftarrow$ C $\left(\hat{j}_i, i\right)$
5: $\hat{Z} \leftarrow \hat{Z} +$ ComCoef
6: **end for**
7: **return** $\hat{Z}$

III. SPECTRAL EFFICIENCY

Spectral efficiency (SE) is an important performance metric in OFDM systems. It is defined as the bit rate that can be achieved within a unit bandwidth B. For the conventional CO-OFDM systems, the spectral efficiency can be given by,

$$SE_{CO-OFDM} = \frac{N_u \log_2 M}{(T_{FFT} + T_{CP})\, B} \tag{15}$$

where N_u is the number of active subcarriers for data transmission in the CO-OFDM systems, and T_{CP} is the time of the cyclic prefix. For the CO-OFDM-IM systems, the spectral efficiency can be expressed as,

$$SE_{CO-OFDM-IM} = \frac{G\left(k \log_2 M + \left\lfloor \log_2(C(n,k)) \right\rfloor\right)}{(T_{FFT} + T_{CP})\, B} \tag{16}$$

Assuming $N_u = N_{FFT} = 256$ and $N_{CP} = 16$, the CO-OFDM system can achieve a SE value 0.9412 bits/s/Hz for BPSK modulation. However, the CO-OFDM-IM system can achieve a SE value 0.9412 bits/s/Hz for $n = 4, k = 2$ and a SE value 1.1765 bits/s/Hz for $n = 4, k = 3$, respectively, for BPSK modulation. Hence, in the CO-OFDM-IM system, the SE value can be achieved higher than that in the CO-OFDM system according to the selected n and k values. So, the proper selection of n and k values can help enhance the SE.

The SE as a function of active subcarrier k is shown under different number of the OFDM subblocks for $M = 2, N_{FFT} = 256, N_{CP} = 16$ and BPSK modulation in Fig. 2. As shown in Fig. 2, when the proper number of the active subcarrier is chosen, the CO-OFDM-IM system can improve SE over the CO-OFDM system.

The CO-OFDM-IM can provide better spectral efficiency than the CO-OFDM at the low-to-medium order modulation such as BPSK, QPSK, and 16QAM as shown in Fig. 3. However, the spectral efficiency of the CO-OFDM-IM cannot compete with that of the CO-OFDM at the high order modulation.

The maximization of SE is almost synonymous with maximizing the number of bits per symbol. The sequence of binomial coefficients $C(n,k)$ is a logarithmically concave sequence. Therefore, it is analytically possible to detect the optimal value of the active subcarrier which maximizes p bits [28].

$$p = k \log_2 M + \left\lfloor \log_2(C(n,k)) \right\rfloor \tag{17}$$

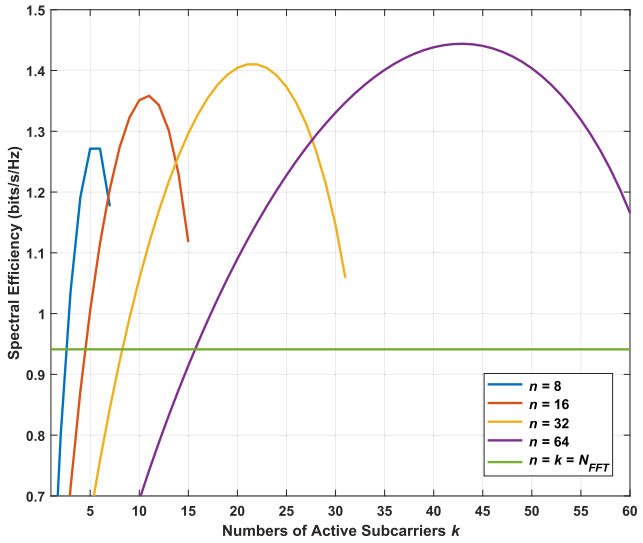

FIGURE 2. Spectral efficiency of the CO-OFDM-IM system for different number of the OFDM subblock.

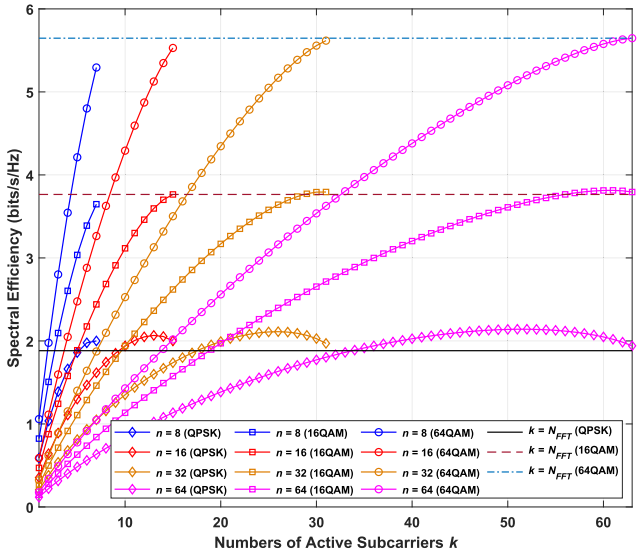

FIGURE 3. Spectral efficiency of the CO-OFDM-IM system for different number of the OFDM subblock.

Assuming dropping the floor function in (17) and then taking its derivative of p with respect to k,

$$\frac{dp}{dk} = \log_2(M) + \log_2\left(\Gamma_{n-k} - \Gamma_k\right) \tag{18}$$

$$\Gamma_k = \sum_{j=1}^{k} \frac{1}{j} = \frac{1}{1} + \frac{1}{2} + \frac{1}{3} + \cdots \frac{1}{k} \tag{19}$$

where the k^{th} harmonic number Γ_k is the sum of the reciprocals of the first k positive integers. Since the limit $\Gamma_k - \log k$ goes to γ which is the Euler-Mascheroni constant, the approximate value of Γ_k is expressed as,

$$\Gamma_k \approx \log k + \gamma \tag{20}$$

By substituting the approximate value of Γ_k in (18) and making (18) equal to zero, it is obtained the optimal number of the active subcarrier,

$$\hat{k} \approx \left\lfloor \frac{MN_{FFT}}{G(M+1)} \right\rfloor \tag{21}$$

IV. AVERAGE BIT ERROR PROBABILITY

Let $\left(X_g \to \hat{X}_g\right)$ denote the pairwise error event that in g^{th} subblock is incorrectly detected. Since the pairwise error events within different subblocks are identical and independent, the pairwise error event within a single subblock is sufficient to determine the OFDM block performance.

In the presence of channel estimation errors in which a mismatched ML detector is used for data detection, the conditional pairwise error probability (CPEP) can be expressed by [9] (22), as shown at the bottom of the page, where σ_e^2 is the estimation error variance of the vector of the channel frequency response H_g, $(\cdot)^H$, $\|\cdot\|$ and $Q(\cdot)$ denote the Hermitian transposition, the Frobenius norm and the Gaussian Q-function, respectively.

$$\begin{aligned}\left\|X_g^H\left(X_g - \hat{X}_g\right)\hat{H}_g\right\|^2 &= \sum_{i=1}^{n} |X_g(i)|^2 \left|\left(X_g(i) - \hat{X}_g(i)\right)\hat{H}_g(i)\right|^2 \\ &= \frac{1}{n}\|X_g\|^2 \left\|\left(X_g - \hat{X}_g\right)\hat{H}_g\right\|^2 \end{aligned} \tag{23}$$

So, the CPEP can be expressed again as

$$\Pr\left(X_g \to \hat{X}_g \middle| \hat{H}_g\right) = Q\left(\sqrt{\frac{\left\|\left(X_g - \hat{X}_g\right)\hat{H}_g\right\|^2}{2\sigma_e^2\|X_g\|^2/n + 2N_0}}\right) \tag{24}$$

Then, the unconditional pairwise error probability (UPEP) can be obtained by

$$\Pr\left(X_g \to \hat{X}_g\right) = E_{\hat{H}_g}\left\{Q\left(\sqrt{\frac{\left\|\left(X_g - \hat{X}_g\right)\hat{H}_g\right\|^2}{2\sigma_e^2\|X_g\|^2/n + 2N_0}}\right)\right\} \tag{25}$$

where $E_{\hat{H}_g}\{\cdot\}$ denotes the expectation operation with respect to the estimated channel frequency response. To obtain the closed-form expression of the UPEP, the approximate Gaussian Q-function can be applied. To enhance the accuracy,

$$\Pr\left(X_g \to \hat{X}_g \middle| \hat{H}_g\right) = Q\left(\frac{\left\|\left(X_g - \hat{X}_g\right)\hat{H}_g\right\|^2}{\sqrt{2\sigma_e^2\left\|X_g^H\left(X_g - \hat{X}_g\right)\hat{H}_g\right\|^2 + 2N_0\left\|\left(X_g - \hat{X}_g\right)\hat{H}_g\right\|^2}}\right) \tag{22}$$

the approximate Gaussian Q-function is proposed in [29], given by

$$Q(x) \approx 0.168e^{-0.876x^2} + 0.144e^{-0.525x^2} + 0.002e^{-0.603x^2}, \quad x > 0 \tag{26}$$

To the approximate UPEP, (26) is applied to (25),

$$\Pr\left(X_g \to \hat{X}_g\right) \approx E_{\hat{H}_g}\{0.168e^{-0.876q\left\|\left(X_g-\hat{X}_g\right)\hat{H}_g\right\|^2} + 0.144e^{-0.525q\left\|\left(X_g-\hat{X}_g\right)\hat{H}_g\right\|^2} + 0.002e^{-0.603q\left\|\left(X_g-\hat{X}_g\right)\hat{H}_g\right\|^2}\} \tag{27}$$

where $q = n\Big/\left(2\sigma_e^2\left\|X_g\right\|^2 + 2nN_0\right)$. Using (27), the expectation can be calculated according to the spectral theorem in [9] and the UPEP upper bound can be calculated as

$$\Pr\left(X_g \to \hat{X}_g\right) \approx \frac{0.168}{\det\left(\mathbf{I}_n + 0.876q\hat{K}_n\mathbf{A}\right)} + \frac{0.144}{\det\left(\mathbf{I}_n + 0.525q\hat{K}_n\mathbf{A}\right)} + \frac{0.002}{\det\left(\mathbf{I}_n + 0.603q\hat{K}_n\mathbf{A}\right)} \tag{28}$$

where $\mathbf{I}_n$ denotes n-dimensional identity matrix. $\hat{K}_n = E\left\{\hat{H}_g\hat{H}_g^H\right\} = \mathbf{K}_n + \sigma_e^2\mathbf{I}_n$ is the correlation matrix of $\hat{H}_g$, $\mathbf{K}_n = E\left\{H_gH_g^H\right\}$ and $\mathbf{A} = \left(X_g - \hat{X}_g\right)^H\left(X_g - \hat{X}_g\right)$. Then, based on the UPEP derived above, an upper bound on the average bit error probability (ABEP) can be obtained as,

$$P_{ABEP} \approx \frac{1}{pn_{X_g}}\sum_{X_g}\sum_{\hat{X}_g}\Pr\left(X_g \to \hat{X}_g\right)e\left(X_g, \hat{X}_g\right) \tag{29}$$

where $e\left(X_g, \hat{X}_g\right)$ represents the number of bit errors for the corresponding pairwise error event and $n_{X_g} = 2^p$ is the number of the possible realizations of X_g.

V. SIMULATION AND DISCUSSION

To investigate the channel impairments of the long-haul coherent optical communication system, the system was installed in the receiver and transmitter shown in Fig. 1 and simulated on the MATLAB platform. The channel block was simulated with the Split-Step Fourier Method (SSFM) for solving NLSE. The SSFM was implemented with a constant step-size criterion and with an FFT size equals to the OFDM frame. This system can be made use of by many applications to simulate impairment such as dispersion effects and fiber nonlinearity in optical communication systems [30].

Optical fiber parameters and OFDM parameters are presented in Table 2 and Table 3 respectively. It is assumed in the simulation that a perfectly synchronized system compensates for carrier frequency offset. The simulations were performed over 500 independent channels. On the transmitter side, the data bits were generated using the Pseudorandom Binary Sequence (PRBS) generator, and then data mapped with the QPSK and 16QAM modulations.

TABLE 2. Fiber optical parameters.

Parameter	Value
Wavelength (λ)	$1550nm$
Chromatic dispersion parameter	$16ps/nm/km$
Nonlinearity coefficient (γ)	$1.32(W.km)^{-1}$
Attenuation (α)	$0.2dB/km$
Noise figure of EDFA	$5dB$
Length of spans	$100km$
Fiber	Standard single mode fiber (SSMF)

TABLE 3. OFDM parameters.

Parameter	Value
FFT/IFFT length (N_{FFT})	256
Cyclic prefix	6.25%
Sampling rate (f_s)	$32GSa/s$
Modulation Type	QPSK and 16QAM

It is well known that the OFDM signal is a high PAPR waveform that requires a large dynamic range of nonlinear devices such as digital-to-analog converters (DACs), power amplifiers, and external optical modulators (Mach-Zehnder Modulator). Also, the high PAPR leads to the increase of nonlinearity of optical fiber. However, the PAPR is ideally required to stay within the linear operating range of nonlinear devices at the transmitter [31]. It has been aimed that the OFDM signal has a low PAPR by using PAPR reduction techniques.

Here, taking into consideration the splitting of a N_{FFT} subcarriers into G subcarrier blocks with k active subcarrier each, the PAPR behavior of the proposed system was analyzed. The PAPR is defined for a transmit signal $v(t)$ as

$$PAPR_{dB} = 10\log_{10}\frac{\max|v(t)|^2}{E\left\{|v(t)|^2\right\}} \tag{30}$$

where $E\{\cdot\}$ represents the expectation or mean value over a sufficient long time period. When the performance for PAPR reduction techniques needs to be evaluated, the complementary cumulative distribution function (CCDF), which is the probability that PAPR exceeds a predefined threshold value $PAPR_0$, is used as [32]

$$CCDF\left(PAPR_{dB}\right) = Prob\left\{PAPR_{dB} > PAPR_0\right\} \tag{31}$$

Fig. 4 shows the CCDFs of PAPR reduction performance of the proposed CO-OFDM-IM with different numbers of active subcarriers and the conventional CO-OFDM. For example, the proposed CO-OFDM-IM with $n = 4$ and $k = 3$ provides about 0.5 dB reduction in PAPR than that of the conventional CO-OFDM at a CCDF value of 10^{-4} for QPSK modulation. At the same CCDF value, the proposed CO-OFDM-IM with BPSK and 16QAM modulation, respectively, achieves about 0.2 dB and 0.4 dB reduction in PAPR. As a result, the partial selection of the active subcarriers in the subcarrier blocks

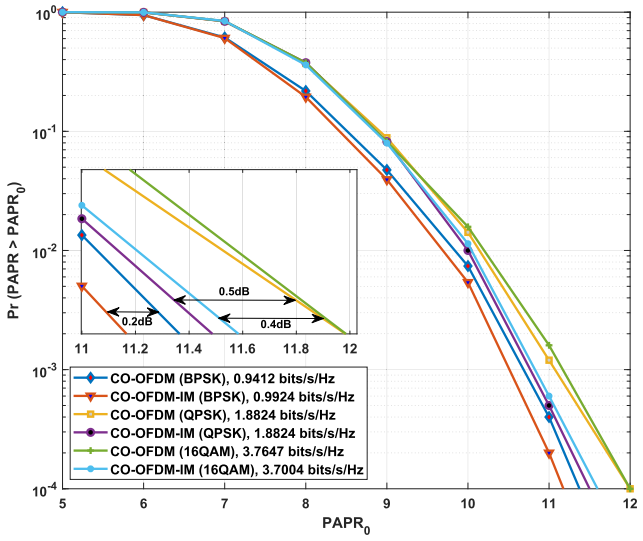

FIGURE 4. PAPR performance of the proposed CO-OFDM-IM and the CO-OFDM systems.

of the proposed CO-OFDM-IM results in a reduction of the PAPR.

In Fig. 5 and Fig. 6, it is compared the BER performance of the proposed CO-OFDM-IM with the CO-OFDM at the different launch power values for QPSK and 16QAM modulation. In Fig. 5 and Fig. 6, both the effect of the launch power and, the effect of the transmission distance are observed, because the effect of the fiber nonlinearity depends on the instantaneous power of the signal and the transmission distance according to NLSE. To evaluate the effect of the fiber nonlinearity only, the laser is assumed to have no phase noise.

At a low launch power, the optical fiber channel can be modeled as a linear dispersive channel impaired by the amplified spontaneous emission (ASE) noise. However, the proposed CO-OFDM-IM performance is lower than the CO-OFDM in low launch power, because the proposed CO-OFDM-IM performance is decreased by the bit errors caused by incorrectly recovered active subcarrier indices. The minimum point of the BER curve is called the optimum launch power. Optimum launch power varies depending on modulation type, transmission distance, and different parameters. The right side of the optimum launch power shows the region where the effect of the fiber nonlinearity is effective. That is, the fiber nonlinearity becomes significant when the launch power increases to allow long-haul transmission. Because the fiber nonlinearity causes randomly a spreading around the central point of each subcarrier leading to adjacent subcarriers interfering with each other.

As shown in Fig. 5 and Fig. 6, the proposed CO-OFDM-IM can provide better BER performance than the CO-OFDM for mid-to-high launch power values where the fiber nonlinearity is effective. The better BER performance of the proposed CO-OFDM-IM can be explained by additional binary bits transmitted by the active subcarrier indices and the higher robustness against inter-carrier interference as a result of the number and the location of the inactive subcarriers. In other words, the CO-OFDM-IM successfully mitigates the effect of the fiber nonlinearity and supports a long-haul transmission.

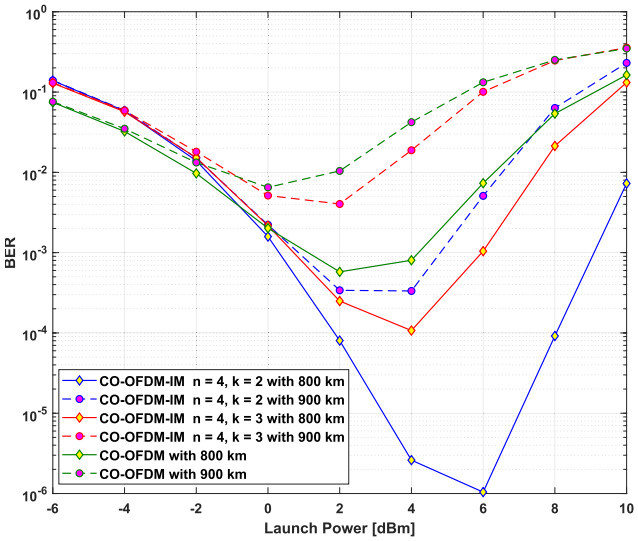

FIGURE 5. BER performance under different launch powers for QPSK modulation after different transmission distance.

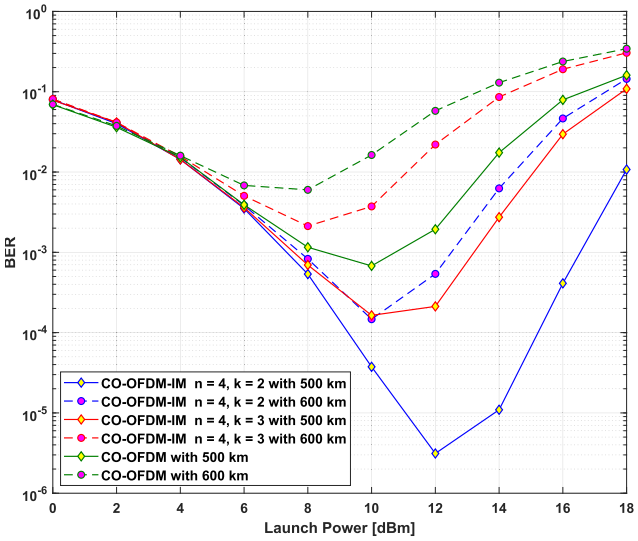

FIGURE 6. BER performance under different launch powers for 16QAM modulation after different transmission distance.

Fig. 7 and Fig. 8 show the BER performance of the proposed CO-OFDM-IM with the CO-OFDM for QPSK and 16QAM modulation at SE levels of 2 bit/s/Hz and 3 bit/s/Hz, respectively. The number of both the subcarriers n and the active subcarriers k in each subblock were chosen to achieve the SE levels as close as possible. As shown in Fig. 7 and Fig. 8, the proposed CO-OFDM-IM outperforms the CO-OFDM at high launch power. For example, for the spectral efficiency value of 1.8824 bits/s/Hz, the proposed CO-OFDM-IM can provide significant BER performance improvement.

Also, the proposed CO-OFDM-IM (8,7) attains 0.12 bit/s/Hz spectral efficiency gain, although it has a similar BER performance as CO-OFDM in the right side of the

optimum launch power as shown in Fig. 7. Considering these achievements, it can be said that the CO-OFDM-IM is capable of taking a good tradeoff between BER performance and spectral efficiency.

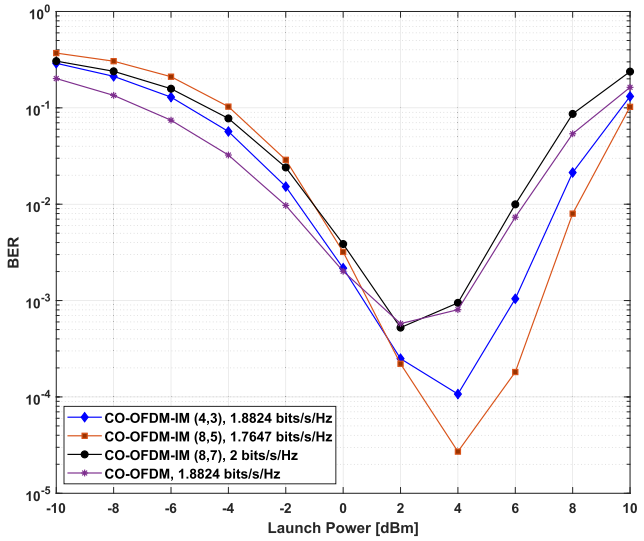

FIGURE 7. Performance comparison between the proposed CO-OFDM-IM and the conventional CO-OFDM for QPSK modulation after 800 km transmission distance.

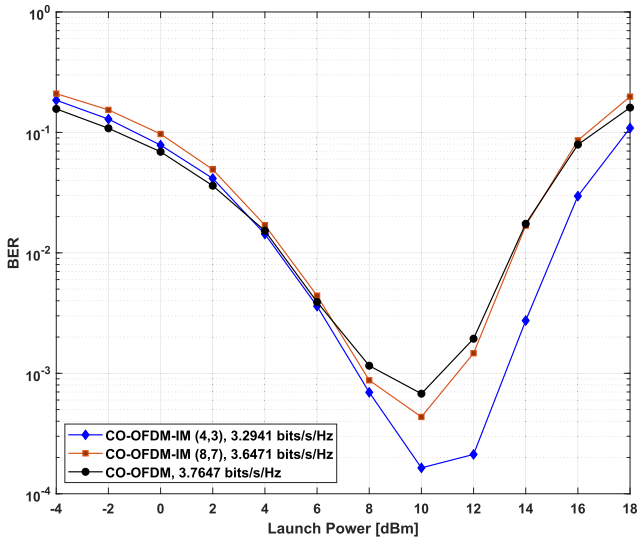

FIGURE 8. Performance comparison between the proposed CO-OFDM-IM and the conventional CO-OFDM for 16QAM modulation after 500 km transmission distance.

Error vector magnitude (EVM) is a useful system-level metric to quantify the impact of the impairments in a system. For coherent optical communication systems, the EVM is commonly used as a measure of the received signal's quality after the channel equalizer. The EVM describes the effective distance of the received complex symbol from its ideal position in the constellation diagram [33].

The performance of average EVM is obtained for launch power = 4dB, 6dB and 8dB to quantify the impact of the linear impairment on subcarriers at a low launch power for 16QAM modulation after 500 km transmission distance. Average EVM is calculated at the receiver for the CO-OFDM and CO-OFDM-IM symbols over 1000 channel realization after the channel equalizer. At each realization, the EVM value on a given subcarrier is the square root of the ratio of the power of the error vector to the average reference constellation power. The performance of the average EVM is shown in Fig. 9 for the CO-OFDM and CO-OFDM-IM. As a result, the average EVMs of CO-OFDM and CO-OFDM-IM are similar in terms of EVM variations over subcarriers at low launch power levels as shown in Fig. 9.

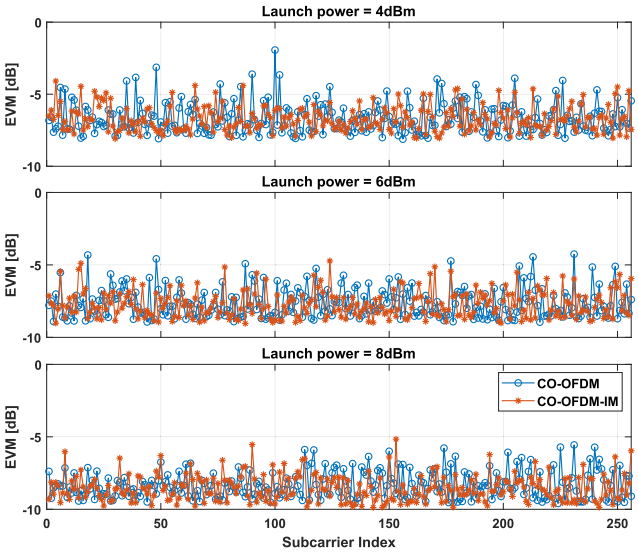

FIGURE 9. EVM versus subcarriers at low launch power levels.

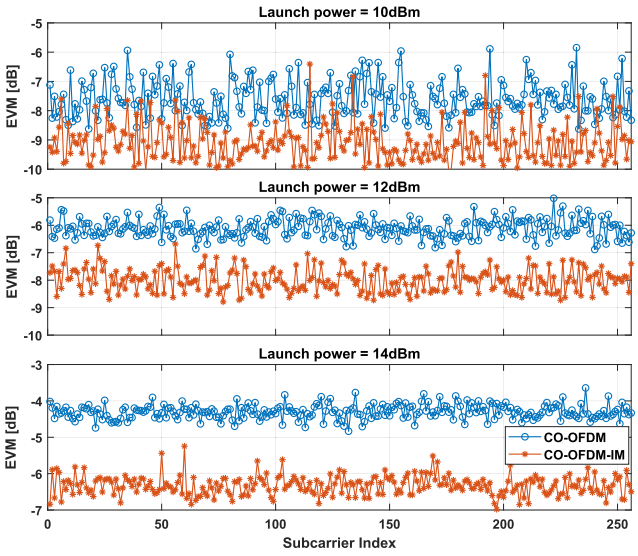

FIGURE 10. EVM versus subcarriers at high launch power levels.

The performance of the average EVM is obtained for launch power = 10dB, 12dB and 14dB to quantify the impact of the nonlinear impairment on subcarriers at mid-to-high launch power values where the fiber nonlinearity is effective.

The performance of the average EVM is shown in Fig. 10 for the CO-OFDM and CO-OFDM-IM.

Comparing CO-OFDM-IM with CO-OFDM, in CO-OFDM-IM system larger average EVM has been observed on the subcarriers as shown in Fig. 10. Since inactive subcarriers don't cause nonlinear interference with adjacent subcarriers, the effect of the fiber nonlinearity on active subcarriers is mitigated.

VI. CONCLUSION

In this paper, it has been introduced the coherent optical OFDM-IM for the long-haul optical communication systems suffering from especially the fiber nonlinearity.

The coherent optical OFDM-IM provides an interesting trade-off between BER and spectral efficiency. Since the number of active subcarriers can be adjusted accordingly to reach the desired spectral efficiency or BER performance, the coherent optical OFDM-IM system can bring important spectral efficiency improvement. Also, the coherent optical OFDM-IM system can provide better BER performance than the coherent optical OFDM systems for mid-to-high launch power values when the proposed CO-OFDM-IM system and the CO-OFDM system have similar spectral efficiency.

The variation of the number and the location of inactive subcarriers directly affects PAPR reduction and is robust to inter-carrier interference.

REFERENCES

[1] T. Tang, X. Zou, P. Li, W. Pan, B. Luo, and L. Yan, "Proposal and demonstration of subcarrier index modulation OFDM for RoF system with enhanced spectral efficiency," *J. Lightw. Technol.*, vol. 36, no. 19, pp. 4501–4506, Oct. 1, 2018.

[2] X. Sun, Z. Zuo, S. Su, and X. Tan, "Blind chromatic dispersion estimation using fractional Fourier transformation in coherent optical communications," in *Proc. IEEE Int. Conf. Artif. Intell. Inf. Syst. (ICAIIS)*, Mar. 2020, pp. 339–342.

[3] M. Chen, J. Yu, and X. Xiao, "Real-time Q-band OFDM-RoF systems with optical heterodyning and envelope detection for downlink transmission," *IEEE Photon. J.*, vol. 9, no. 2, pp. 1–7, Apr. 2017.

[4] S. N. Thool, D. Chack, and A. Kumar, "Coherent detection-based optical OFDM, 60 GHz radio-over-fiber link using frequency quadrupling, and channel and carrier phase estimation," *Frontiers Phys.*, vol. 9, p. 504, Oct. 2021. [Online]. Available: https://www.frontiersin.org/article/10.3389/fphy.2021.749497

[5] J. S. Ferreira *et al.*, "GFDM frame design for 5G application scenarios," *J. Commun. Inf. Syst.*, vol. 32, no. 1, pp. 54–61, 2017. [Online]. Available: https://jcis.sbrt.org.br/jcis/article/view/432

[6] F. Di Stasio, M. Mondin, and F. Daneshgaran, "Multirate 5G downlink performance comparison for f-OFDM and w-OFDM schemes with different numerologies," in *Proc. Int. Symp. Netw., Comput. Commun. (ISNCC)*, Jun. 2018, pp. 1–6.

[7] J. Abdoli, M. Jia, and J. Ma, "Filtered OFDM: A new waveform for future wireless systems," in *Proc. IEEE 16th Int. Workshop Signal Process. Adv. Wireless Commun. (SPAWC)*, Jun. 2015, pp. 66–70.

[8] E. Ozturk, E. Basar, and H. A. Cirpan, "Generalized frequency division multiplexing with flexible index modulation," *IEEE Access*, vol. 5, pp. 24727–24746, 2017.

[9] E. Başar, U. Aygölü, E. Panayırcı, and H. V. Poor, "Orthogonal frequency division multiplexing with index modulation," *IEEE Trans. Signal Process.*, vol. 61, no. 22, pp. 5536–5549, Nov. 2013.

[10] M. Di Renzo, H. Haas, A. Ghrayeb, S. Sugiura, and L. Hanzo, "Spatial modulation for generalized MIMO: Challenges, opportunities, and implementation," *Proc. IEEE*, vol. 102, no. 1, pp. 56–103, Jan. 2014.

[11] M. C. Gursoy, E. Basar, A. E. Pusane, and T. Tugcu, "Index modulation for molecular communication via diffusion systems," *IEEE Trans. Commun.*, vol. 67, no. 5, pp. 3337–3350, May 2019.

[12] C. Sacchi, T. Rahman, I. A. Hemadeh, and M. El-Hajjar, "Millimeter-wave transmission for small-cell backhaul in dense urban environment: A solution based on MIMO-OFDM and space-time shift keying (STSK)," *IEEE Access*, vol. 5, pp. 4000–4017, 2017.

[13] E. Basar and E. Panayirci, "Optical OFDM with index modulation for visible light communications," in *Proc. 4th Int. Workshop Opt. Wireless Commun. (IWOW)*, Sep. 2015, pp. 11–15.

[14] T. Mao, R. Jiang, and R. Bai, "Optical dual-mode index modulation aided OFDM for visible light communications," *Opt. Commun.*, vol. 391, pp. 37–41, May 2017.

[15] A. W. Azim, Y. Le Guennec, M. Chafii, and L. Ros, "Enhanced optical-OFDM with index and dual-mode modulation for optical wireless systems," *IEEE Access*, vol. 8, pp. 128646–128664, 2020.

[16] Y. Deng, S. Wu, X. Liu, D. Li, J. Jiao, and Q. Zhang, "Index modulated polar codes," in *Proc. IEEE Wireless Commun. Netw. Conf. (WCNC)*, May 2020, pp. 1–6.

[17] T. Mao, Z. Wang, Q. Wang, S. Chen, and L. Hanzo, "Dual-mode index modulation aided OFDM," *IEEE Access*, vol. 5, pp. 50–60, 2017.

[18] S. A. Çolak, Y. Acar, and E. Basar, "Adaptive dual-mode OFDM with index modulation," *Phys. Commun.*, vol. 30, pp. 15–25, Oct. 2018.

[19] Y. Acar and T. Cooklev, "High performance OFDM with index modulation," *Phys. Commun.*, vol. 32, pp. 192–199, Feb. 2019.

[20] R. Fan, Y. J. Yu, and Y. L. Guan, "Generalization of orthogonal frequency division multiplexing with index modulation," *IEEE Trans. Wireless Commun.*, vol. 14, no. 10, pp. 5350–5359, May 2015.

[21] Y. Xiao, S. Wang, L. Dan, X. Lei, P. Yang, and W. Xiang, "OFDM with interleaved subcarrier-index modulation," *IEEE Commun. Lett.*, vol. 18, no. 8, pp. 1447–1450, Aug. 2014.

[22] J. Choi, "Coded OFDM-IM with transmit diversity," *IEEE Trans. Commun.*, vol. 65, no. 7, pp. 3164–3171, Jul. 2017.

[23] E. Basar, M. Wen, R. Mesleh, M. Di Renzo, Y. Xiao, and H. Haas, "Index modulation techniques for next-generation wireless networks," *IEEE Access*, vol. 5, pp. 16693–16746, 2017.

[24] A. D. Ellis, M. E. McCarthy, M. A. Z. Al Khateeb, M. Sorokina, and N. J. Doran, "Performance limits in optical communications due to fiber nonlinearity," *Adv. Opt. Photon.*, vol. 9, no. 3, pp. 429–503, Sep. 2017.

[25] S. Queiroz, J. P. Vilela, and E. Monteiro, "Optimal mapper for OFDM with index modulation: A spectro-computational analysis," *IEEE Access*, vol. 8, pp. 68365–68378, 2020.

[26] M. Seimetz, *High-Order Modulation for Optical Fiber Transmission* (Springer Series in Optical Sciences). Berlin, Germany: Springer, 2009. [Online]. Available: https://books.google.it/books?id=xP05eLvfTtAC

[27] A. J. Lowery, "Fiber nonlinearity mitigation in optical links that use OFDM for dispersion compensation," *IEEE Photon. Technol. Lett.*, vol. 19, no. 19, pp. 1556–1558, Oct. 1, 2007.

[28] A. W. Azim, M. Chafii, Y. Le Guennec, and L. Ros, "Spectral and energy efficient fast-OFDM with index modulation for optical wireless systems," *IEEE Commun. Lett.*, vol. 24, no. 8, pp. 1771–1774, Aug. 2020.

[29] T. Mao, Q. Wang, J. Quan, and Z. Wang, "Zero-padded orthogonal frequency division multiplexing with index modulation using multiple constellation alphabets," *IEEE Access*, vol. 5, pp. 21168–21178, 2017.

[30] C.-P. Ma and J.-W. Kuo, "Orthogonal frequency division multiplex with multi-level technology in optical storage application," *Jpn. J. Appl. Phys.*, vol. 43, no. 7B, pp. 4876–4878, Jul. 2004, doi: 10.1143/jjap.43.4876.

[31] S. Amiralizadeh, A. T. Nguyen, and L. A. Rusch, "Modeling and compensation of transmitter nonlinearity in coherent optical OFDM," *Opt. Exp.*, vol. 23, no. 20, pp. 26192–26207, Oct. 2015.

[32] S. Litsyn, *Peak Power Control in Multicarrier Communications*. Cambridge, U.K.: Cambridge Univ. Press, 2007.

[33] C. Goken and O. Dizdar, "Performance of edge windowing for OFDM under non-linear power amplifier effects," in *Proc. IEEE Mil. Commun. Conf. (MILCOM)*, Oct. 2017, pp. 219–224.

AHMET GÜNER received the B.S., M.S., and Ph.D. degrees from the Department of Electrical and Electronics Engineering, Karadeniz Technical University, in 2000, 2004, and 2013, respectively. His research interests include wireless communications, signal processing, blind equalization, blind estimation techniques, OFDM, and optical communications systems.